Measurement of metastable lifetimes for transitions in Fe^{9+}, Fe^{10+}, and Fe^{13+}

S. J. Smith, A. Chutjian, and J. A. Lozano
Jet Propulsion Laboratory, California Institute of Technology, Pasadena, California 91109, USA
(Received 28 September 2005; published 15 December 2005)

Radiative lifetimes are measured for metastable levels in the iron charge states Fe^{9+}, Fe^{10+}, and Fe^{13+}. The ions are generated in a 14 GHz electron cyclotron resonance ion source and trapped in a Kingdon ion trap. The Fe levels and their measured lifetimes are (a) 73.0±0.8 ms for the $3s^23p^4(^3P)3d\ ^4F_{7/2}$ level in Fe^{9+}, (b) 9.91±0.5 ms for the $3s^23p^4\ ^1D_2$ level in Fe^{10+}, and (c) 17.0±0.2 ms for the $3s^23p\ ^2P^o{}_{3/2}$ level in Fe^{13+}. Comparisons are made to other measured results using a Kingdon trap, an ion storage, and an electron-beam ion trap (EBIT).

DOI: 10.1103/PhysRevA.72.062504 PACS number(s): 32.70.Cs, 34.80.Kw, 39.10.+j

I. INTRODUCTION

The detection of rich iron line spectra in stellar objects by the space x-ray spectrometers aboard the Chandra [1] and XMM-Newton [2] spacecraft has added new impetus and relevance to the measurement of fundamental atomic-physics properties in all Fe charge states. Transitions in Cl-like Fe^{9+} have been analyzed for abundances in stellar coronae [3], in the solar active region and flares [4]; and emission line ratios have been used as diagnostics of electron density N_e in solar and stellar regions [5]. Metastable transitions in Fe^{10+} (S-like) appear in the wavelength region 100–300 nm, are found most prominently in the solar spectrum [6,7], and can be used to identify nonthermal turbulence in the solar corona [8]. Transitions in Fe^{13+} (Al-like) are found in more energetic solar and stellar flares [9], stellar chromospheres [10], as well as in tokamak plasmas [11].

Of the many atomic parameters required for describing the emissions [12], the measurement of lifetimes of metastable levels (together with excitation cross sections) allows one to establish a line intensity ratio between a forbidden and an allowed transition. This ratio can then be used as a diagnostic of the electron density N_e and temperature T_e in a solar, stellar, or fusion plasma if the level energies, radiative transition rates, and collision strengths are known [13,14]. Given this relevance and importance for solar, stellar, and fusion plasma studies, measurements of lifetimes were undertaken for transitions from excited levels in Fe^{9+} ($^4F_{7/2}$), Fe^{10+} ($^1D_2$), and Fe^{13+} ($^2P^o{}_{3/2}$). Lifetimes for these levels have been previously reported using a Kingdon ion trap [15,16], an electron-beam ion trap (EBIT) [17], and an ion storage ring [18]. In an effort to resolve differences among experiments and results of theoretical calculations, new measurements have been carried out herein using a Kingdon ion trap under ultrahigh vacuum conditions, with good control over systematic and statistical uncertainties.

Details of the experimental approach using the electron cyclotron resonance ion source and Kingdon trap at the Jet Propulsion Laboratory Highly Charged Ion Facility are given in Sec. II. The data acquisition methods and analysis of the lifetime decay curves are given in Sec. III. Also given therein are the present results, with comparisons to other measurements and calculations of the lifetimes for the same Fe^{9+}, Fe^{10+}, and Fe^{13+} transitions.

II. EXPERIMENTAL METHODS

Partial energy diagrams for the relevant levels in the iron charge states are shown in Figs. 1–3 for Fe^{9+}, Fe^{10+}, and Fe^{13+}, respectively. The Fe level symmetries and energies are taken from the compilations of Refs. [19,20]. Experimental measurements are carried out using the 14 GHz electron cyclotron resonance ion source (ECRIS) [21]. The iron ions are generated using ferrocene vapor in the plasma chamber. The ions are extracted from the ECRIS at a potential of 6.4 kV. They are then mass-charge selected, directed into the beam line containing the Kingdon ion trap, and focused into the trap [22]. The trap is turned "on" by rapidly pulsing the central wire within the trap cylinder from its nontrapping potential of 6.4 to 3 kV. Simultaneously, the upstream ions are rapidly deflected away from the focusing lens system, so that no additional ions or ion-generated background particles can enter the trap during the photon decay cycle [23]. The ions settle into orbits about the central wire within a time of less than 2 ms. While orbiting, they emit radiation at wavelength corresponding to the various Fe transitions, at a decay

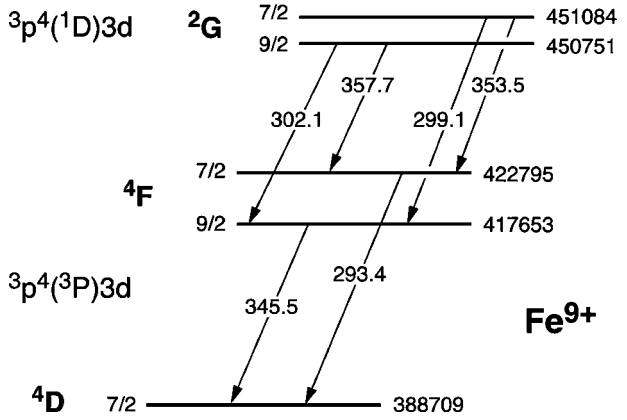

FIG. 1. Partial energy level diagram of Fe^{9+} indicating the measured 293.4 nm emitting line from the $^4F_{7/2}$ level. A shorter decay constant corresponding to the lifetime of the $^2G_{7/2,9/2}$ levels arises through partial transmission by the interference filter of the 299.1 and 302.1 nm emission lines from those levels. Numbers in the diagram within arrows are wavelengths in nanometers, and numbers to the right of each level are energies in centimeters^{-1}.

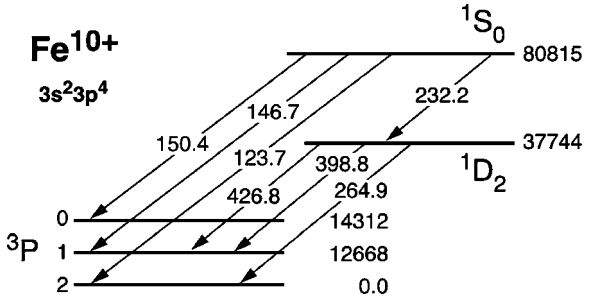

FIG. 2. Partial energy-level diagram of Fe^{10+}, indicating the measured 264.9 nm emission line from the $^1D_2$ level.

rate given by the inverse lifetime of the upper level (provided that long-lived cascading transitions into the initial state are absent or negligible). The population in the upper level is also lost via ion-background gas collisional-quenching, charge exchange collisions of the ion with the background gas, and by collisions with the central wire and walls.

The photon detector and interference filter are exterior to the fused quartz window of the vacuum chamber. A positively biased mesh in front of the photon-collection optics prevents ions from hitting the first lens surface and causing fluorescence. A single uv-grade, solar-blind photomultiplier is used in the ultraviolet measurements for Fe^{9+} and Fe^{10+}; and an optical-grade photomultiplier is used in the Fe^{13+} work. The detectors are operated in a pulse-counting mode, with the output pulses amplified and counted with a PC-based multichannel scaler. The time resolution was 0.1 ms/channel, with a 2 s sampling window. These values can be conveniently changed in the sampling card hardware for work with longer or shorter lifetimes. The range of lifetimes that can be measured is determined, at the short end, by the time it takes for ions to settle into stable orbits ($\sim$1–2 ms), and at the long end by the trap lifetime ($\sim$1.7 s), as governed by the loss mechanisms mentioned above. The trap is filled and emptied every 2 s. This is sufficient to allow one to fit a trap lifetime line shape on each of the decay curves. The results have been accumulated over a 1 yr period, interspersed with electron excitation and charge exchange measurements on the other JPL beam lines. Typically, about 50 h of sampling time for each decay curve is required to accumulate good statistics. In separate measurements, a channel electron multiplier (CEM) plate detector

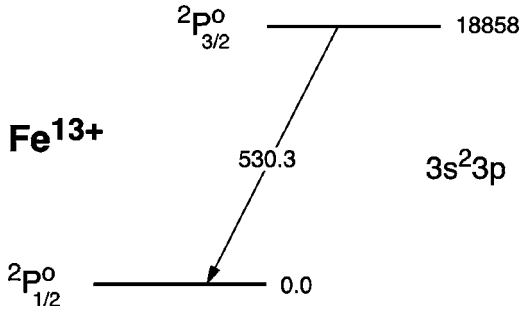

FIG. 3. Energy-level diagram for Fe^{13+} showing the ground-state coronal green line transition at 530.3 nm.

was used to count ions after an adjustable trap "dump" time, so as to measure the ion-trapping population as a function of trap load time. Trap lifetimes and trap rates (R_{trap}) obtained in this way were consistent with the photon-decay line shapes (1200–1700 ms).

III. MEASUREMENT RESULTS AND DISCUSSION

Presented in the following is a description of the experimental techniques used for each charge state, the expression governing the experimental fluorescence decay rate, and the signal and background levels encountered. For each ion, results of the present measurements, together with previous measurements by others using an ion storage ring, electron-beam ion trap (EBIT), and a Kingdon trap are given in Table I. Also presented in Table I are the results of a number of theoretical calculations of the level lifetimes.

A. The Fe^{9+}, $3s^23p^4(^3P)3d\ ^4F_{7/2}$ level

A partial energy-level diagram of the transitions in Fe^{9+} is shown in Fig. 1. The lifetime measurement of the metastable $^4F_{7/2}$ level was carried out using a 295 ± 5.5 nm (FWHM) bandwidth. The fluorescence decay $F(t)$ was fitted to a constant background plus a three-term exponential decay modulated by the trap decay rate, all given by

$$F(t) = S_0 + \left\{ \sum_{j=1}^{2} S_j e^{-A_j t} + B_g \right\} e^{-R_{\text{trap}} t} + S_3 e^{-R_3 t}. \qquad (1)$$

The modulating factor $\exp(-R_{\text{trap}}t)$ describes the effect of ions being lost from the trap due to inhomogeneous trapping fields and ion-background gas collisions. The constant term B_g represents photons within the filter bandwidth that are generated by ion-surface effects, such as ions hitting the trap walls, the central wire, or the quartz lens. The decay term $S_3\exp(-R_3t)$ describes the brief instability ($\sim$1 ms) of the trap immediately after loading as ion orbits stabilize. The constant S_0 describes the dark current of the multiplier phototube. In the Fe^{9+} measurements S_j and A_j ($j=1$, 2) are, respectively, the amplitudes and rates for the unresolved $^4F_{7/2}$-$^2G_{7/2,9/2}$ transitions, and for the resolved $^4D_{7/2}$-$^4F_{7/2}$ transition. Values of A_1 and A_2 were obtained with fitted time constants of 18.3 and 70.0 ms, respectively.

The shorter of the two decay constants (A_1) consists of the $^4F_{9/2}$-$^2G_{7/2}$ transition (Fig. 1, 299.1 nm) with a calculated branching ratio of 0.11 and a theoretical upper limit to the lifetime of 20.6 ms [27]. The nearby $^4F_{9/2}$-$^2G_{9/2}$ transition (302.1 nm) has an upper level lifetime of 17.8 ms [24]. Accurate results for the $^4F_{9/2}$-$^2G_{7/2,9/2}$ transitions cannot be obtained from the present data due to the large statistical error and the unknown nature of the ^2G blend; however a lifetime of $\sim$18 ms was measured for the combined $^4F_{7/2}$-$^2G_{7/2,9/2}$ decays.

The longer of the two decay constants (A_2) is assigned to the $^4D_{7/2}$-$^4F_{7/2}$ transition (293.4 nm) with a theoretical branching ratio of $\sim$0.55. For the sake of clarity an estimate of the dark current parameter S_o was obtained by examining the decay curves at large times ($>$1.5 s) from the trap-

TABLE I. Summary of experimental and theoretically-calculated lifetimes for the metastable levels in Fe^{9+}, Fe^{10+}, and Fe^{13+} studied herein. The acronyms to the theoretical methods are CB=Coulomb-Born, CI=Configuration Interaction (with the number of states given in parentheses), DW=Distorted Wave, MCDF =Multiconfiguration Dirac-Fock, MHFR=Relativistic Multiconfiguration Hartree-Fock, and TF=Thomas Fermi.

Ion	Level (emission wavelength)	Lifetime (ms)	Type of Trap	Reference
		experimental		
Fe^{9+}	$3s^2 3p^4(^3P)3d\ ^4F_{7/2}$ (293.4 nm)	70.0±0.8	Kingdon	this work
		93±30	Kingdon	[24]
		58±10	Storage ring	[18]
Fe^{10+}	$3s^2 3p^4\ ^1D_2$ (264.9 nm)	9.91±0.5	Kingdon	this work
		9.86±0.22	Kingdon	[16]
		11.05±0.1	Storage ring	[18]
Fe^{13+}	$3s^2 3p^2 P^o_{3/2}$ (530.3 nm)	17.0±0.2	Kingdon	this work
		17.52±0.29	Kingdon	[15,16]
		18.0±1.2	Storage ring	[18]
		16.74±0.12	EBIT	[17,25]
		Results of theoretical calculations		
Ion	Level	Lifetime (ms)	Theory	Reference
Fe^{9+}	$3s^2 3p^4(^3P)3d\ ^4F_{7/2}$	66.2	TF	[26]
		80.4	CI (4)	[27]
		80.0	CI($\leqslant$2025)	[24]
		77.27	Grasp	[28]
Fe^{10+}	$3s^2 3p^4\ ^1D_2$	10.5	CI (4)	[29]
		12.8	TF	[26]
		9.84	CI (8)	[30]
		9.80	HFR	[31]
		11.9	MCDF	[32]
		9.81	CI (4)	[33]
		10.8	CI($\leqslant$2025)	[16]
		10.82	Superstructure	[34]
		10.9	MCDF	[35]
Fe^{13+}	$3s^2 3p\ ^2P^o_{3/2}$	16.58	Scaled TF	[36]
		16.6	HF(from [38])	[37]
		16.65	HF	[38]
		16.60	CB	[39]
		16.65	Compiled data	[40]
		16.6	Compiled data	[41]
		19.6	MHFR	[42]
		16.66	MCDF	[43]
		16.6	Compiled data	[44]
		16.51	HFR	[45]
		16.6	MCDF	[20]
		21.38	DW	[46]
		17.01	CI($\leqslant$2025)	[16]

loading time. This value was then subtracted from each channel of the decay curve.

The final fitting parameters in Eq. (1) are S_o=0 (suppressed to zero for clarity in the plotted data), S_1=44.77, S_2=339.7, R_{trap}=0.833 s^{-1}, B_g=21.17, R_3=270 s^{-1}, and S_3=2214.8. Results of the fit to the data are given as the solid curve in Fig. 4. Shown in the lower panel are the residual counts (fitted minus signal counts) along the time axis. The lifetime of the $^4F_{7/2}$ level is 70.0±0.8 ms (1σ). This value lies between results in two other measurements of 93±30 ms

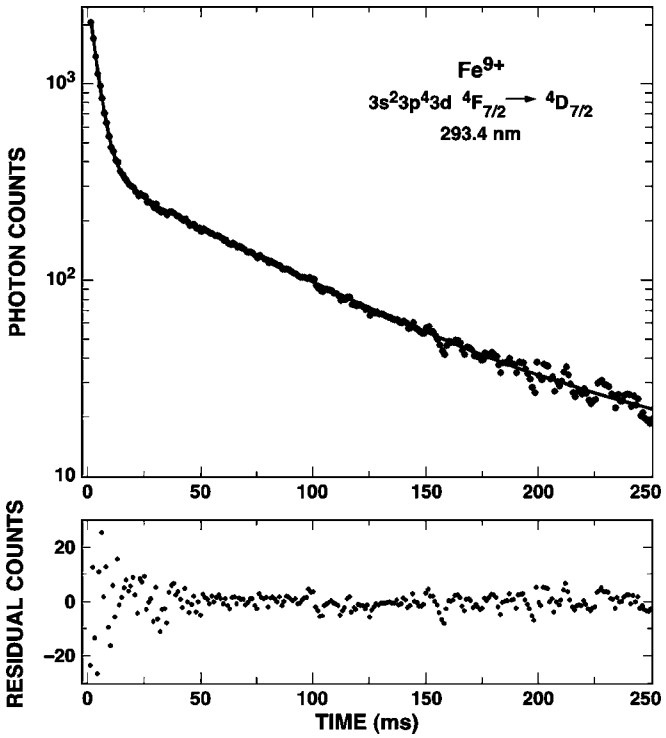

FIG. 4. Photon decay rate for the Fe^{9+} $3s^2 3p^4(^3P)3d\ ^4F_{7/2} \rightarrow {}^4D_{7/2}$ transition at 293.4 nm. The decay time constant is 73.0±0.8 ms. The residuals of the fit (calculated fit minus data) are shown for each measurement bin.

(Kingdon trap) and 58±10 ms (storage ring) and also lies amidst results in three calculations of 80.4, 80.0, and 66.2 ms (see Table I).

B. The Fe^{10+}, $3s^2 3p^4\ ^1D_2$ level

The metastable $^1D_2$ level decays through the two M1 transitions to the $^3P_2$ and $^3P_1$ levels. The lifetime of the $^1D_2$ level was measured via the 264.9 nm radiation in the $^3P_2$ -$^1D_2$ transition (Fig. 2). Assuming a statistical weight for the population of the sublevels within the ground term, ~33% of the stored ions should be in the $^1D_2$ level. Contribution to this population from the cascading ^1S_o level is expected to be negligible due to a less than 1% branching ratio in the $^1D_2$–^1S_o line, and the relatively small ^1S_o level population. Observations were made of the $^3P_2$-$^1D_2$ transition using a 265±6 nm [full width at half maximum (FWHM)] interference filter. This filter rejected the $^1D_2$-^1S_o emission at 232.2 nm.

The governing equation for the decay is

$$F(t) = S_0 + \{S_1 e^{-A_1 t} + B_g\} e^{-R_{\text{trap}} t} + S_3 e^{-R_3 t}. \quad (2)$$

A three-term exponential fit included an $R_3{}^{-1}=1$ ms trap settling time, and an $R_{\text{trap}}{}^{-1}=1400$ ms trap lifetime. The final fitting parameters in Eq. (2) are $S_o=0$ (suppressed to zero for clarity in the plotted data), $S_1=1004.6$, $R_{\text{trap}}=0.714\ \text{s}^{-1}$, $B_g=21.17$, $R_3=270\ \text{s}^{-1}$, and $S_3=2214.8$. Results for the data fitting are given as the solid line in Fig. 5, with the residual counts shown in the panel below. The measured lifetime is

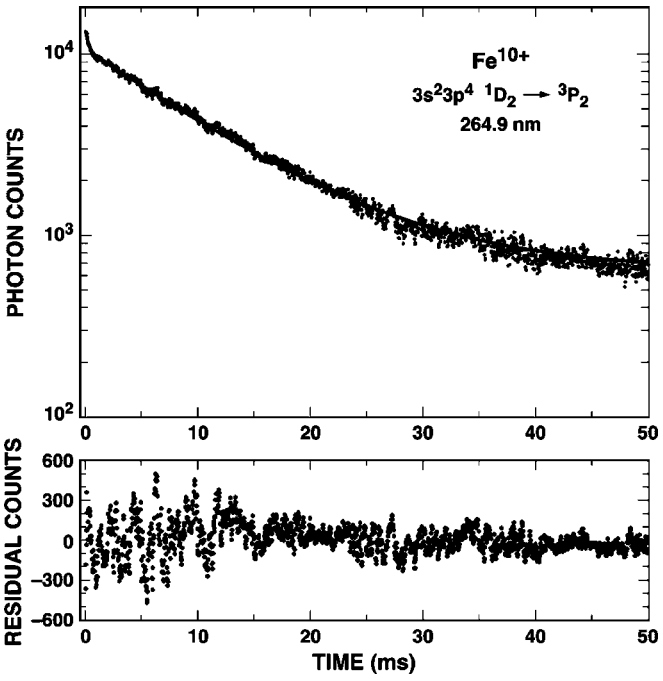

FIG. 5. Photon decay rate for the Fe^{10+} $3s^2 3p^2 3p^4\ ^1D_2 \rightarrow {}^3P$ transition at 264.9 nm. The decay time constant for the $^1D_2$ level is 9.91±0.5 ms.

9.91±0.5 ms. This compares favorably with a previous Kingdon-trap measurement (9.86±0.22 ms), but lies well below a storage-ring measurement of 11.05±0.1 ms. Comparisons to theory are generally satisfactory, with a number of the theoretical results lying within the error limits of the measurement (Table I).

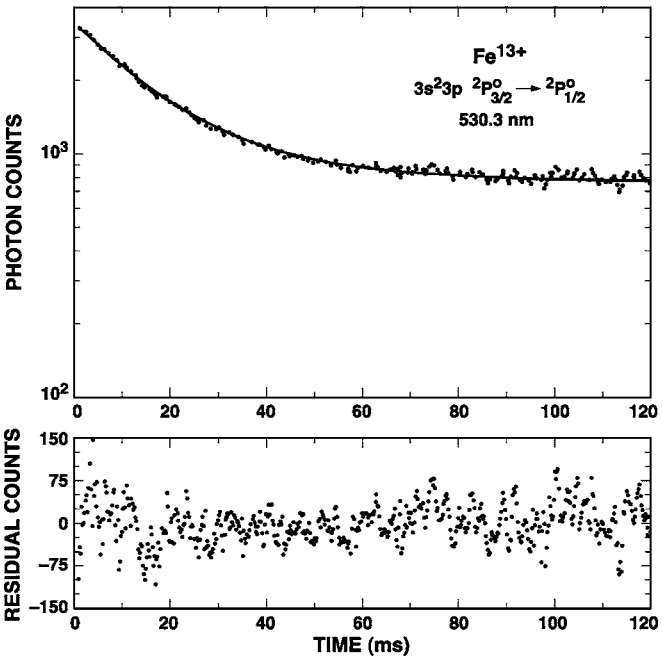

FIG. 6. The photon decay rate for the Fe^{13+} ground state, coronal green line transition $3s^2 3p^2 P^o{}_{3/2} \rightarrow {}^2P^o{}_{1/2}$ at 530.3 nm. The measured lifetime is 17.0±0.2 ms.

There are additional transitions from the metastable $^1G_4{}^o$, $^3G_4{}^o$, and $^3F_4{}^o$ levels that lie in the vicinity of 264.9 nm [18,26,35], with calculated lifetimes in the range 16–80 ms [18]. Interferences to the lifetime fitting from these levels can be ruled out in the present work since (i) the line emissivities are low relative to that of the $^1D_2$ transition, and (ii) the wavelengths lie outside the 259–271 bandwidth of the filter used herein [26,35]. However, some of these transitions are transmitted within the optical bandwidth (160–280 nm) used for the storage-ring measurements [18]. And, hence, part of the difference in measured lifetimes (9.91 ms versus 11.05 ms) could be in the use (present case) of a narrower photon energy range that allows one to systematically limit the number of decay curves present. A remeasurement of this lifetime on the storage ring using a narrowband 265 nm filter to isolate just the strongest $^3P_2$-$^1D_2$ transition would be helpful.

C. Fe^{13+}, $3s^23p\ ^2P^o_{3/2}$ level

The energy levels for the Fe^{13+} ground fine-structure splitting are shown in Fig. 3. The coronal green line at 530.3 nm was isolated using an interference filter centered near 530±5 nm (FWHM). A three-term exponential fit to the data was made through Eq. (2).

As noted above, an optical-grade PM tube with somewhat larger dark current was used in the Fe^{13+} coronal green line measurements. A slightly greater trap settling signal (the S_3 and R_3 parameters) was also measured for this ion. Hence, it was decided to truncate the decay data curve for the first 1 ms to allow for a better fit to the trap settling counts. This 1 ms truncation also gave rise to a somewhat smoother appearance at the beginning.

The final fitting parameters for Fe^{13+} from Eq. (2) are $S_o=16.06$, $S_1=2684.1$, $R_1=58.1\ s^{-1}$, $R_{trap}=0.585\ s^{-1}$, $B_g=811.3$, $R_3=667\ s^{-1}$, and $S_3=3.12$. Results for the data fitting are given as the solid line in Fig. 6, with the residual counts shown in the panel below. The measured lifetime of the $^2P^o_{3/2}$ level is 17.0±0.2 ms. This compares very well with two other measurements of 17.52±0.29 (Kingdon trap) [15,16] and 16.74±0.12 ms (EBIT) [17,25]. All measurements used a 530 nm isolation filter. The storage ring result of 18.0±1.2 ms [18] is inconclusive, as that measurement suffered from a low ring flux of Fe^{13+} ions; and a low signal/background level arising from the use of a 530 nm (green) isolation filter followed by a red-sensitive phototube. A new storage-ring measurement of this transition rate would be most useful. A number of theoretical calculations give results clustered in the range 16.5–17.0 ms, in good agreement with the present results and those of Refs. [15–17,25]. All data are summarized in Table I.

ACKNOWLEDGMENTS

We acknowledge D. Church for equipment and for helpful technical discussions. J. Lozano thanks the National Research Council for support through the NASA-NRC program. This work was carried out at the Jet Propulsion Laboratory, California Institute of Technology, and was supported through the National Aeronautics and Space Administration.

[1] Y. Krongold, F. Nicastro, M. Elvis, N. C. Brickhouse, S. Mathur, and A. Zezas, Astrophys. J. **620**, 165 (2005).
[2] A. J. J. Raassen, R. Mewe, M. Audard, M. Güdel, E. Behar, J. S. Kaastra, R. L. J. Van der Meer, C. R. Foley, and J-U. Ness, Astron. Astrophys. **389**, 228 (2002).
[3] J. D. Drake, J. M. Laming, and K. G. Widing, Astrophys. J. **443**, 393 (1995);J. M. Laming, J. D. Drake, and K. G. Widing, Astrophys. J. **443**, 416 (1995).
[4] J. W. Brosius, J. M. Davila, and R. J. Thomas, Astrophys. J., Suppl. Ser. **119**, 255 (1998).
[5] V. J. Foster, M. Mathioudakis, F. P. Keenan, J. J. Drake, and K. G. Widing, Astrophys. J. **473**, 560 (1996).
[6] G. D. Sandlin and R. Tousey, Astrophys. J. **227**, L107 (1979).
[7] G. D. Sandlin, J.-D. F. Bartoes, G. E. Brueckner, R. Tousey, and M. E. VanHoosier, Astrophys. J., Suppl. Ser. **61**, 801 (1986).
[8] U. Feldman and G. A. Doschek, J. Opt. Soc. Am. **67**, 726 (1977).
[9] P. Quinet, Phys. Scr. **61**, 452 (2000).
[10] E. Landi, M. Landini, and G. Del Zanna, Astron. Astrophys. **324**, 1027 (1997).
[11] R. U. Datla, J. R. Roberts, R. D. Durst, W. L. Hodge, C. C. Klepper, W. L. Rowan, and J. B. Mann, Phys. Rev. A **36**, 5448 (1987).
[12] A. Chutjian, in *The Physics of Multiple and Highly Charged Ions*, edited by F. J. Currell (Kluwer, Dordrecht, 2003), Ch. 3.
[13] F. P. Keenan, in *UV and X-Ray Spectroscopy of Laboratory and Astrophysical Plasmas*, edited by E. H. Silver and S. M. Khan (Cambridge University Press, Cambridge, England, 1993), p. 44.
[14] J. P. Lynch and M. Kafatos, Astrophys. J., Suppl. Ser. **76**, 1169 (1991).
[15] D. P. Moehs and D. A. Church, Astrophys. J. **516**, L111 (1999).
[16] D. P. Moehs, M. I. Bhatti, and D. A. Church, Phys. Rev. A **63**, 032515 (2001).
[17] P. Beiersdorfer, E. Träbert, and E. H. Pinnington, Astrophys. J. **587**, 836 (2003)
[18] E. Träbert, G. Gwinner, A. Wolf, E J. Knystautas, H-P. Garnir, and X. Tordoir, J. Phys. B **35**, 671 (2002).
[19] C. Corliss and J. Sugar, J. Phys. Chem. Ref. Data **11**, 135 (1982).
[20] J. R. Fuhr, G. A. Martin, and W. L. Wiese, J. Phys. Chem. Ref. Data **17**, 1 (1988).
[21] A. Chutjian, J. B. Greenwood, and S. J. Smith, in *Applications of Accelerators in Research and Industry*, edited by J. L. Duggan and I. L. Morgan (AIP, New York, 1999), p. 881.
[22] S. J. Smith, I Čadež, A. Chutjian, and M. Niimura, Astrophys. J. **602**, 1075 (2004).
[23] S. J. Smith, A. Chutjian, and J. B. Greenwood, Phys. Rev. A

60, 3569 (1999).
[24] D. P. Moehs, D. A. Church, M. I. Bhatti, and W. F. Perger, Phys. Rev. Lett. **85**, 38 (2000).
[25] E. Träbert, Astron. Astrophys. **415**, L39 (2004).
[26] H. E. Mason and H. Nussbaumer, Astron. Astrophys. **54**, 547 (1977).
[27] A. K. Bhatia and G. A. Doschek, At. Data Nucl. Data Tables **60**, 97 (1995).
[28] K. M. Aggarwal and F. P. Keenan, Astron. Astrophys. **427**, 763 (2004).
[29] J. M. Malville and R. A. Berger, Planet. Space Sci. **13**, 1131 (1965)
[30] C. Mendoza and C. J. Zeippen, Mon. Not. R. Astron. Soc. **202**, 981 (1983).
[31] E. Biémont and J. E. Hansen, Phys. Scr. **34**, 116 (1986)
[32] E. B. Salomon and Y-K. Kim, At. Data Nucl. Data Tables **41**, 339 (1989).
[33] A. K. Bhatia and G. A. Doschek, At. Data Nucl. Data Tables **64**, 183 (1996).
[34] A. K. Bhatia, G. A. Doschek, and W. Eissner, At. Data Nucl. Data Tables **82**, 211 (2002).
[35] S. Fritzsche, C. Z. Dong, and E. Träbert, Mon. Not. R. Astron. Soc. **318**, 263 (2000).
[36] B. Warner, Z. Astrophys. **69**, 399 (1968).
[37] M. W. Smith and W. L. Wiese, J. Phys. Chem. Ref. Data **2**, 85 (1973).
[38] S. J. Czyzak, L. H. Aller, and R. N. Euwema, Astrophys. J., Suppl. Ser. **28**, 465 (1974);T. K. Krueger and S. J. Czyzak, Mem. R. Astron. Soc. **69**, 145 (1965).
[39] S. O. Kastner, Sol. Phys. **46**, 179 (1976).
[40] M. Kafatos and J. P. Lynch, Astrophys. J., Suppl. **42**, 611 (1980).
[41] M. Eidelsberg, F. Crifo-Magnant, and C. J. Zeippen, Astron. Astrophys. **43**, 455 (1981).
[42] C. Froese-Fischer and B. Liu, At. Data Nucl. Data Tables **34**, 261 (1983).
[43] K.-N. Huang, At. Data Nucl. Data Tables **34**, 1 (1986).
[44] V. Kaufman and J. Sugar, J. Phys. Chem. Ref. Data **15**, 321 (1986).
[45] E. Biémont, R. D. Cowan, and J. E. Hansen, Phys. Scr. **37**, 850 (1988)
[46] A. K. Bhatia and S. O Kastner, J. Quant. Spectrosc. Radiat. Transf. **49**, 609 (1993).